JOURNAL OF CHROMATOGRAPHY A

Journal of Chromatography A, 887 (2000) 367–378

www.elsevier.com/locate/chroma

Improved column preparation and performance in capillary electrochromatography

Erdmann Rapp, Ernst Bayer*

Research Center of Nucleic Acid and Peptide Chemistry, Institut für Organische Chemie, Universität Tübingen, Auf der Morgenstelle 18, D-72076 Tübingen, Germany

Abstract

Problems encountered in capillary electrochromatography, i.e. non-reproducible column manufacture, bubble formation during usage, short column lifetimes and limited choice of packing particles are addressed by the development of fritless or single-frit, internally tapered, segmented and dead-volume free coupled capillary columns. The Van Deemter plots measured demonstrate the performance of these high-quality capillaries which are suitable for capillary electrochromatography as well as for capillary high-performance liquid chromatographic applications.

Keywords: Fritless packed capillaries; Column design; Tapers; Capillary electrochromatography

1. Introduction

Capillary electrochromatography (CEC) has emerged as a promising, highly efficient new technique for the separation of neutral and charged compounds [1,2].

Since the flow is generated electrokinetically, the flow profile has plug-form at distances from the wall in excess of approximately the electrical double layer thickness. Furthermore, since the electroosmotic flow is theoretically independent of the particle size down to particle diameters (d_p) of 0.4 μm [1,3], small particles (e.g. 1.5 μm) with their inherently higher separation efficiency can be readily used. As has been demonstrated, plate numbers up to 700 000/m could be generated using 1.5-μm particles [3–8]. From a more practical point of view, pressurised CEC (pCEC) offers advantages, especially for gradient elution [9], and on-line coupling to MS [10] and NMR [11].

Nonetheless, CEC has not yet found wide routine application. The reasons for this lie among others in technical problems associated with CEC:

1. Poor reproducibility of the mechanical properties of sintered frits which retain the stationary phase in the capillary.
2. Non uniformity of the stationary phase surface caused by the sintering process which can lead to destruction of an otherwise successful separation.
3. Bubble formation caused by insufficiently degassed mobile phases, structural inhomogeneities inside the outlet frit and the excessive pressure drop at the end of this frit [12].
4. The fragility of the UV-detection window which shortens the average lifetime of electrochromatography capillaries.
5. Limitations on the choice of packing materials imposed by the necessity to form frits with the

*Corresponding author. Tel.: +49-7071-297-437; fax: +49-7071-295-034.

0021-9673/00/$ – see front matter
PII: S0021-9673(99)01208-X

packing (e.g. organic polymer beads and chiral phases are unsuitable).

Several proposals have been made to overcome these difficulties [3,4,12–14]. One of these is the avoidance of frits, especially with particles smaller than 3 μm, since here frit preparation is troublesome. Whereas bubble formation and destruction of separation can be avoided by a single-frit system the use of polymer beads requires a completely fritless capillary column set-up. It has been shown [5,15–17] that by means of internal or external tapers in the fused-silica capillaries, particles with significantly smaller diameter than the orifice of the taper can be successfully retained as a result of the so-called keystone effect, obviating the need for a frit. It was also shown [5,16] that 10 μm I.D. internal double tapers upstream of a detection window or correspondingly narrow restrictor capillaries are able to retain 3-μm packing material. With the configurations described however, the replacement of a broken UV detection window is not possible.

Since the UV detection window and the outlet frit are the most fragile parts of the chromatographic system, it is desirable to decouple the packed capillary from the detection segment by way of a robust, dead-volume free, easily replaceable connector. However, the solutions hitherto described have shown deficiencies, namely: pressure was restricted to 6 bar [18], limitations were placed upon the electric field strength because of current leakage [4] and the connectors were not consistently dead-volume free [18].

All these approaches focus only on one or two of the above mentioned difficulties. In addition the numerical limits of the ratio of orifice to particle diameter conducive to the keystone effect have not been studied in detail.

It was our intention to develop a combination of fritless capillary columns and replaceable, directly coupled UV detection cells suitable also for hyphenation of CEC, pCEC [9] and CHPLC with NMR spectroscopy [11,19–21] and Coordination Ionspray-MS (CIS-MS) [22].

In this paper we describe both single-frit and and completely fritless capillary column set-ups with dead-volume free, replaceable connection of the UV detection segment. Detailed procedures for the preparation are given and the performance of representative capillary columns has been studied by means of their Van Deemter plots. In contrast to the configurations reported in the literature [4,5,16,18], this column configuration is both versatile and pressure stable and can be alternatively used for CEC, pCEC and CHPLC.

2. Experimental

2.1. Apparatus and equipment

Fused-silica capillaries with 20, 30, 50, 75, 100 and 150 μm I.D. were purchased from Polymicro Technologies (Phoenix, AZ, USA) and MicroQuartz (München, Germany). All capillary columns were packed with 3 μm Grom-Sil ODS-O AB reversed-phase particles with 100 Å pore size, kindly donated by Grom (Herrenberg, Germany), using a HPLC packing pump (Shandon, Astmoor, UK). The internal tapers were made with a microflame torch Model B (Microflame Limited, Minneapolis, MN, USA). The tapered and non-tapered capillary end-pieces were ground on a grinding machine (Buehler Metaserv (Grinder-Polisher) Buehler UK Coventry, UK) with 5-μm grain-size silicon carbide wet grinding paper P 4000 (Wirtz-Buehler GmbH, Düsseldorf, Germany). The PTFE–FEP dual shrink-tube was used as coupling device because it showed a high mechanical and electrical resistance (a kind gift of IFK-Isofluor (Neuss, Germany), cat. no.: IS 036, expanded I.D.: 0.91 mm, shrunk I.D.: 0.00 mm, wall thickness after shrinkage: 0.60 mm).

All CEC experiments were performed with a P/ACE capillary electrophoretic system MDQ (Beckman Instruments, Fullerton, CA, USA).

2.2. Chemicals and solutions

Gradient grade acetone, methanol, acetonitrile and isopropanole were purchased from Merck (Darmstadt, Germany). Purified water was provided by a MilliQ185 Plus water purification system (Millipore, Eschborn, Germany). Sodium tetraborate and the hydrochloric acid were obtained from Fluka (Buchs, Switzerland). Aqueous sodium tetraborate buffer solution was prepared at 5.0 m*M* concentration and adjusted to a pH of 9.0 with 1.0 *M* and 0.1 *M* HCl.

The thoroughly degassed mobile phase consisted of acetonitrile–aqueous sodium tetraborate buffer (80:20, v/v) solution. The benzoate test mixture (50 m*M* thiourea, 20 m*M* methyl-, 25 m*M* ethyl-, 30 m*M* propyl-, 35 m*M* butyl- and 40 m*M* pentylbenzoate in the above mobile phase) was a gift from Grom (Herrenberg, Germany). All solvents, buffer solutions and mixed mobile phases were filtered over disposable 0.2 μm Chromafil filters (Macherey-Nagel, Düren, Germany).

3. Procedures

3.1. Preparation of the tapered and non-tapered capillary end-pieces

The internal tapers were prepared similarly to the method described by Lord et al. [15] and Choudhary et al. [16]. A fused-silica capillary of double the necessary length was fused at the centre with a microflame torch to form a sealed internal double taper (Fig. 2a). Two internally tapered capillary pieces were formed by cutting the seal at the centre. The tapered ends (and other capillary ends intended to be joined) were held in place by means of PEEK ferrules in a stainless steel block. This enabled the end surfaces to be accurately ground perpendicular to the capillary axis and to create an orifice of the desired diameter (5–45 μm). In this way it is possible to prepare robust thick-walled internal tapered tips using 365 μm O.D. capillaries. The roughness of the capillary end-surface depends on the mode of its preparation as depicted in Fig. 1. A surface quality as shown in Fig. 1c (achieved with P 4000 abrasive) is necessary in order to avoid dead-volumes at the coupling region and to enable the application of pressures up to 550 bar.

3.2. Manufacturing the single-frit capillary columns

The single-frit capillary column consists of two pieces (packed bed and detection capillary), in which the packed capillary segment is tapered and needs no outlet frit. Capillaries of 50–150 μm I.D. were packed using the principle of slurry packing first described for capillary columns by Smith and Evans [13] and later modified by other groups [2,4,12,14]. The manufacturing procedure for single-frit capillary columns is shown schematically in Fig. 2. First, the smoothly ground end of the detection capillary and the ground tapered end of the capillary to be packed are aligned and pushed together carefully with a laboratory-built device allowing positioning in the *x*, *y* and *z* axes (Fig. 2b). During the slurry preparation, (Fig. 2c) a 5-mm piece of the dual PTFE–FEP shrink-tube connector is slipped over the junction and heated to 330°C with a hot air stream. Under these conditions, the inner FEP tube melted while the outer PTFE tube shrank tightly onto the aligned capillary ends. The capillary is then slurry-packed (Fig. 2d) and the inlet frit sintered using a heater with a temperature controlled heating filament (Fig. 2e). Finally, a detection window is prepared by burning or scratching off the polyimide coating at the desired position (Fig. 2f) and the capillary column (Fig. 2i) conditioned (Fig. 2g) or stored for later use (Fig. 2h).

3.3. Manufacturing the fritless capillary columns

The fritless capillary columns can be prepared either as two-piece — packed bed and detection capillary (Fig. 3h), or three-piece — packed bed, tapered retaining and detection capillary (Fig. 3i) units. These capillaries have inlet and outlet tapers and need no retaining frits.

The manufacturing procedure for two-piece fritless capillary columns (Fig. 3a–g) is similar to that for single-frit capillary columns with the exception that these capillary columns are slurry packed before coupling the segments by shrinkage coating. After packing, the column is reversed such that the retaining internal orifice now forms the inlet retainer while an external second taper placed at the coupling end of the detection segment serves as outlet retainer. In this way, no frit sintering was necessary.

The manufacturing procedure for three-piece fritless capillary columns is virtually the same (Fig. 3i). Here however, the outlet retainer and UV detection functions are decoupled by the use of two segments. With this fritless three-piece capillary column design (and also with the two-piece single-frit design), the UV detection segment can easily be exchanged upon

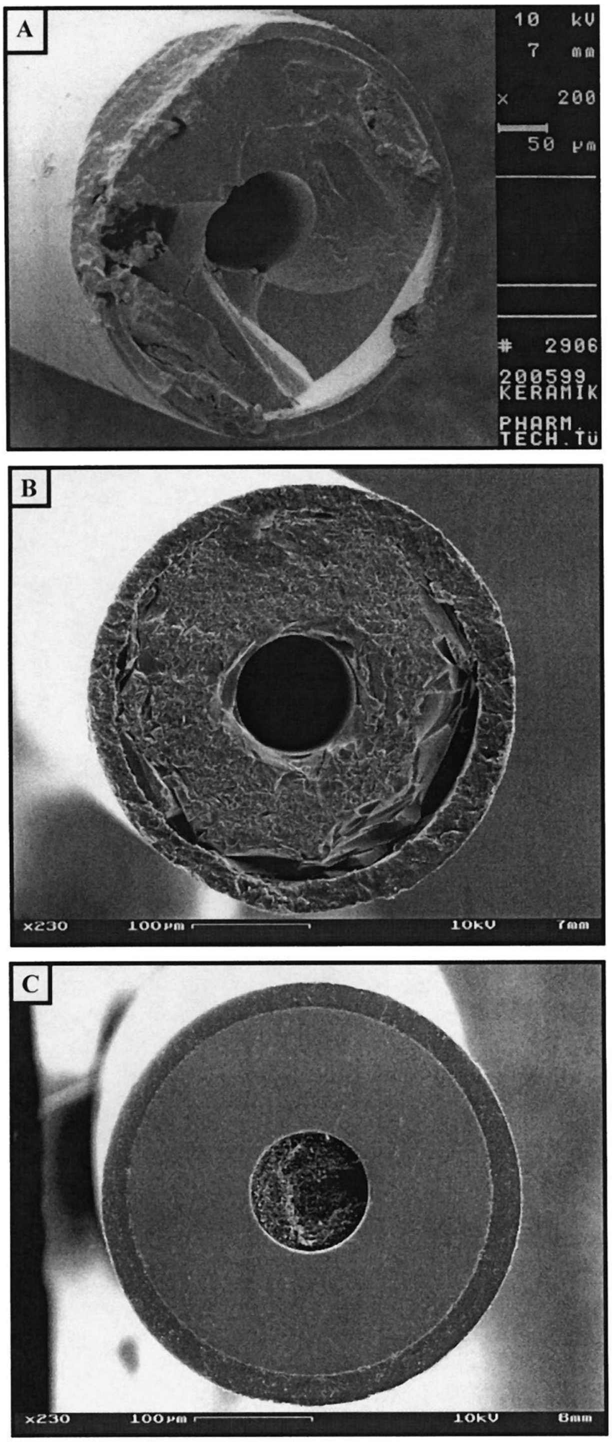

Fig. 1. Scanning electron micrographs (SEM) of fused-silica capillaries with different cross-sectional surface qualities. (A) Cross-sectional surface of a capillary cut with a ceramic tile. (B) Cross-sectional surface of a capillary prepared with silicon carbide wet grinding paper P 320. (C) Cross-sectional surface of a capillary prepared with silicon carbide wet grinding paper P 4000.

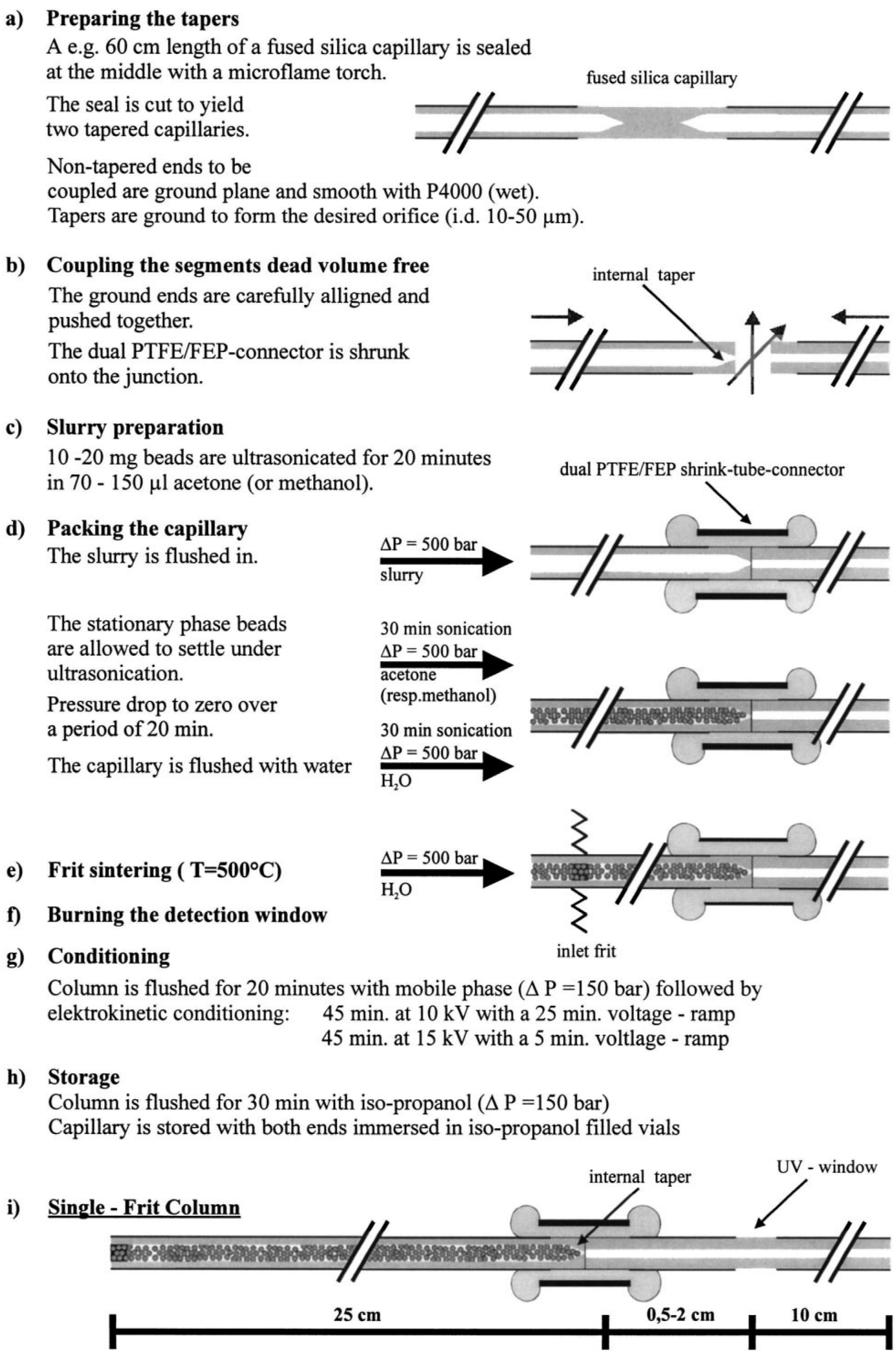

Fig. 2. Successive steps of the manufacturing procedure for single-frit capillary columns.

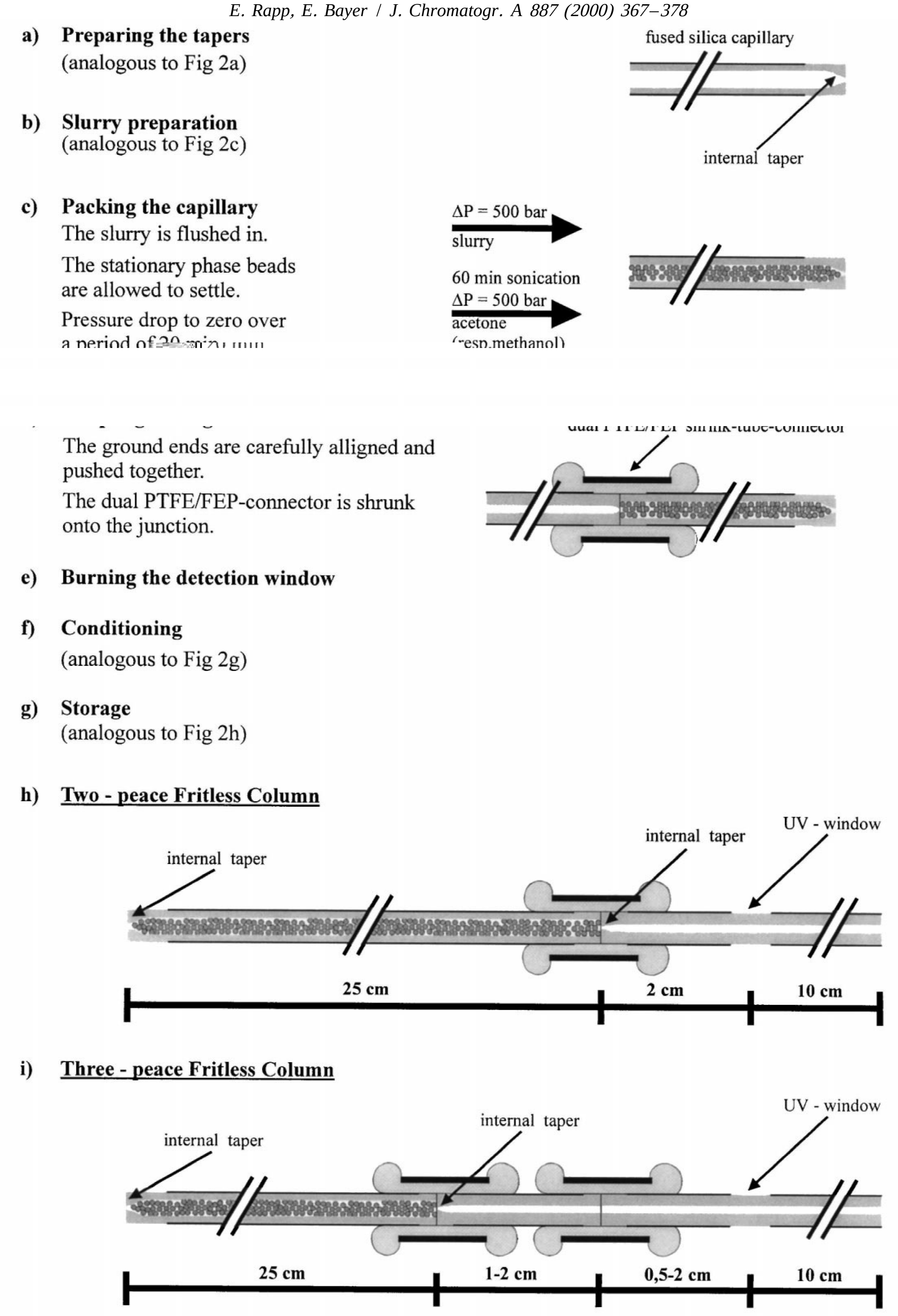

Fig. 3. Successive steps of the manufacturing procedure for fritless capillary columns.

breakage etc. without affecting the quality of the packed bed.

3.4. Degassing and electrochromatography

Insufficient degassing of the mobile phase may lead to an unstable current and even breakdown of electroosmotic flow as a result of bubble formation. In a laboratory-made dispenser, the filtered mobile phases were degassed by purging with helium followed by ultrasonication under vacuum and then stored under a helium atmosphere. Immediately prior to use, the buffer vials were filled via a tap connected to the mobile phase reservoir. Renewed degassing was not necessary. The separations were performed at 30°C under isocratic conditions.

4. Results and discussion

4.1. Properties of internal taper, capillary end surface and capillary column connection

The range of orifice diameter of the internal taper relative to the particle diameter conducive to the keystone effect was first investigated. It was found that for 3-μm beads, the packed bed was reliably retained with an orifice diameter of up to 25 μm and in some cases up to 35 μm, i.e. more than ten times the particle diameter. On the other hand, with internal taper I.D.s smaller than 10 μm, trouble was always encountered with blockage during flushing or drying of the capillaries for the slurry packing. The optimum I.D. of an internal taper for 3 μm packing material is thus 15–25 μm. Tapers in this range allow generation of packed beds showing good long-term stability (over at least 100 runs). Silica-based 1.5-μm particles are retained by internal tapers of up to 16 μm while 6 μm PS–DVB particles are retained by tapers of up to 45 μm I.D..

We also investigated the capillary wall thickness required to form a robust taper. For capillaries with the standard O.D. of 365 μm, the maximum practicable internal diameter was found to be 150 μm; tubes with larger I.D.s tended to break easily.

The surface smoothness should be as shown in Fig. 1c. With rougher surfaces it was not possible to reproducibly manufacture dead-volume free, pressure-stable (up to at least 550 bar) columns. In Fig. 4, such a capillary connection is shown.

Other PTFE connectors tested did not satisfy the requirements. Capillary couplings with non-shrinking PTFE tubes (O.D. 1.6 mm, I.D. 0.3 mm) were not pressure-stable and not always dead-volume free, while the capillary couplings with single PTFE shrink-tubes (O.D. 0.8 mm, I.D. 0.5 mm) were not mechanically stable.

4.2. Optimisation of I.D. in respect to flow velocity and band broadening

Bubble formation can occur at the packed bed end [1,13], where a pressure gradient exists between the packed and the open segment. There a frit can also act as a nucleation site. In these capillary column set-ups without any outlet frit a UV detection segment which acts simultaneously as restrictor capillary decreases the pressure gradient over the coupling region. The I.D. of the UV detection segment was selected to correspond to the interparticulate crossection of the packed capillary segment. The external porosity of a random loose packing [23] is about 0.4, and this value was subsequently used to calculate the corresponding open tube diameters.

Experiments indicated that the optimum open tube diameter is somewhat smaller than that calculated. For this reason the next smaller commercially available capillary I.D. (denoted $\mathrm{I.D.}_{\mathrm{practicable}}$) was chosen (Table 1).

Larger diameters led to increased plate heights and steeper curvature in the Van Deemter plots (Fig. 5a). This additional band broadening is attributed to the pressure drop at the end of the outlet frit as a result of mismatched cross-sectional areas [24] and also possibly turbulent flow. The increased plate heights are not a result of poorer packing as was proved by corresponding measurements after exchanging only the UV detection segment for one with a narrower internal diameter (Fig. 5b).

With this optimised I.D., the pressure drop was negligible and both bubble formation and additional band spreading were suppressed without leading to a reduction of the EOF velocity. This is also shown for a single-frit capillary column with 150 μm I.D. packed bed segment and a 75 μm I.D. UV detection

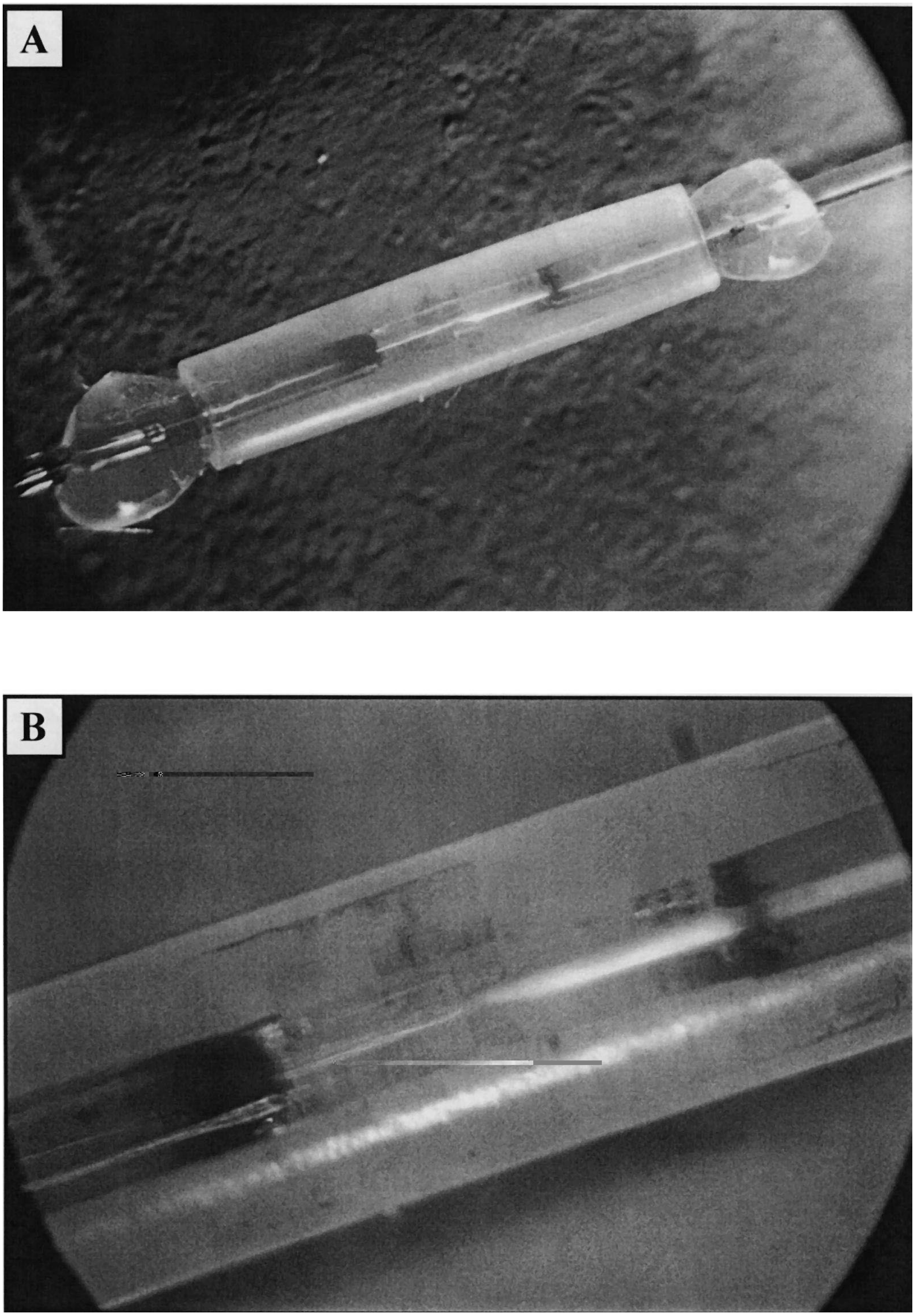

Fig. 4. Photomicrographs of a dead-volume free shrinkage coating connection. (A) Magnified 18 times (B) magnified 67 times.

Table 1
Parameters used to calculate the optimum I.D.s of the UV detection capillary corresponding to the interparticulate cross-sectional area of a random loose packing of packed capillary segments and listed practically used I.D.s[a]

I.D. $_{100\%}$ (μm)	$\varnothing_{100\%}$ (μm^2)	$\varnothing_{40\%}$ (μm^2)	I.D.$_{40\%}$ (μm)	I.D.$_{practicable}$ (μm)
250	49 087.40	19 634.95	158.12	150
180	25 466.90	10 178.80	113.84	100
150	17 671.46	7068.58	94.86	75
100	7853.98	3141.59	63.24	50
75	4417.86	1767.15	47.44	30
50	1963.50	785.40	15.81	10

[a] I.D. $_{100\%}$ = internal diameter of the packed capillary segment. $\varnothing_{100\%}$ = Cross-section of the packed capillary segment. $\varnothing_{40\%}$ = Interparticulate cross-sectional area assuming random loose packing. I.D. $_{40\%}$ = Internal diameter of the UV detection capillary segment with cross-section corresponding to $\varnothing_{40\%}$. I.D. $_{practicable}$ = Next smaller commercially available fused-silica capillary, relative to I.D. $_{40\%}$.

segment (Fig. 5c). No difference was apparent when the UV detection occured 0.5 or 2.0 cm downstream of the retaining outlet taper of the packed bed segment (compare Fig. 5b and d) when using this pressure-matched coupled capillary column set-up.

Using capillaries with 10, 20 and 30 μm I.D. as UV detection capillary segment, no taper was found to be necessary to retain the packing material at the outlet of the packed bed segment. Lower EOF velocities were however incurred when capillaries significantly narrower than the calculated optimum I.D. were used. For example, when 20 or 30 μm I.D. capillaries were coupled to a 100 μm I.D. packed bed segment, 3.0 or 1.5 times lower flow-rates respectively were observed compared to that of the pressure-matched (50/100 μm coupled) capillary column set-up. It seems that unfavourable back pressure in the open segment decreases the EOF velocity within the packed segment. Van Deemter plots of a non-tapered single-frit capillary column with 100 μm I.D. packed bed segment and a 30 μm I.D. UV detection segment are shown in Fig. 5e. The increased plate height observed may be a result of disturbed plug-flow profiles due to the increased back pressure or of an asymmetrical laboratory made UV-bubble-cell which was necessary for these small-diameter detection capillaries. Preliminary tests using these capillary columns in CHPLC revealed no loss in flow velocities using smaller I.D.s for the UV detection segment. It appears that the EOF cannot overcome higher hydrostatic back pressures.

4.3. Comparison of various capillary column designs

The efficiency of an optimised single-frit column set-up is in general equal to or better than that of standard double-frit CEC columns. Reduced plate heights of down to 1.57 (corresponding to 212 000 N/m for 3-μm beads) are easily reached (Fig. 5b and c).

The fritless column design allows the manufacture of columns with excellent performance. The efficiency of these high-quality capillaries is demonstrated with a number of Van Deemter plots and reduced plate heights down to 1.44 (232 000 N/m with 3-μm beads) are readily attained (Fig. 5f). The performance of such a fritless capillary column is demonstrated in the separation of five benzoates shown in Fig. 6. Both single-frit and fritless columns are quite robust. Once conditioned properly, more than 100 separations were performed with good reproducibility. With both the single-frit and the fritless three-piece capillary column design, the UV detection segment could also be easily exchanged without affecting the quality of the packed bed so that there is no need to pack a new column if the detection window breaks.

With these new capillary column constructions, problems associated with the frit reproducibility and its structural inhomogeneities no longer arise. The fritless capillary column design also allows in principle the use of polymer-based beads. It is no longer necessary to retain the beads between silica-based sintered frits, a practice which invariably leads to peak tailing or in the worst case to complete degradation of the separation.

5. Conclusions

With this technique, problems associated with frit reproducibility and its structural inhomogeneities no longer arise. Coupling is performed without introduction of any dead-volume. With both the single-frit and the fritless three-piece capillary column design, the UV detection segment can also be easily ex-

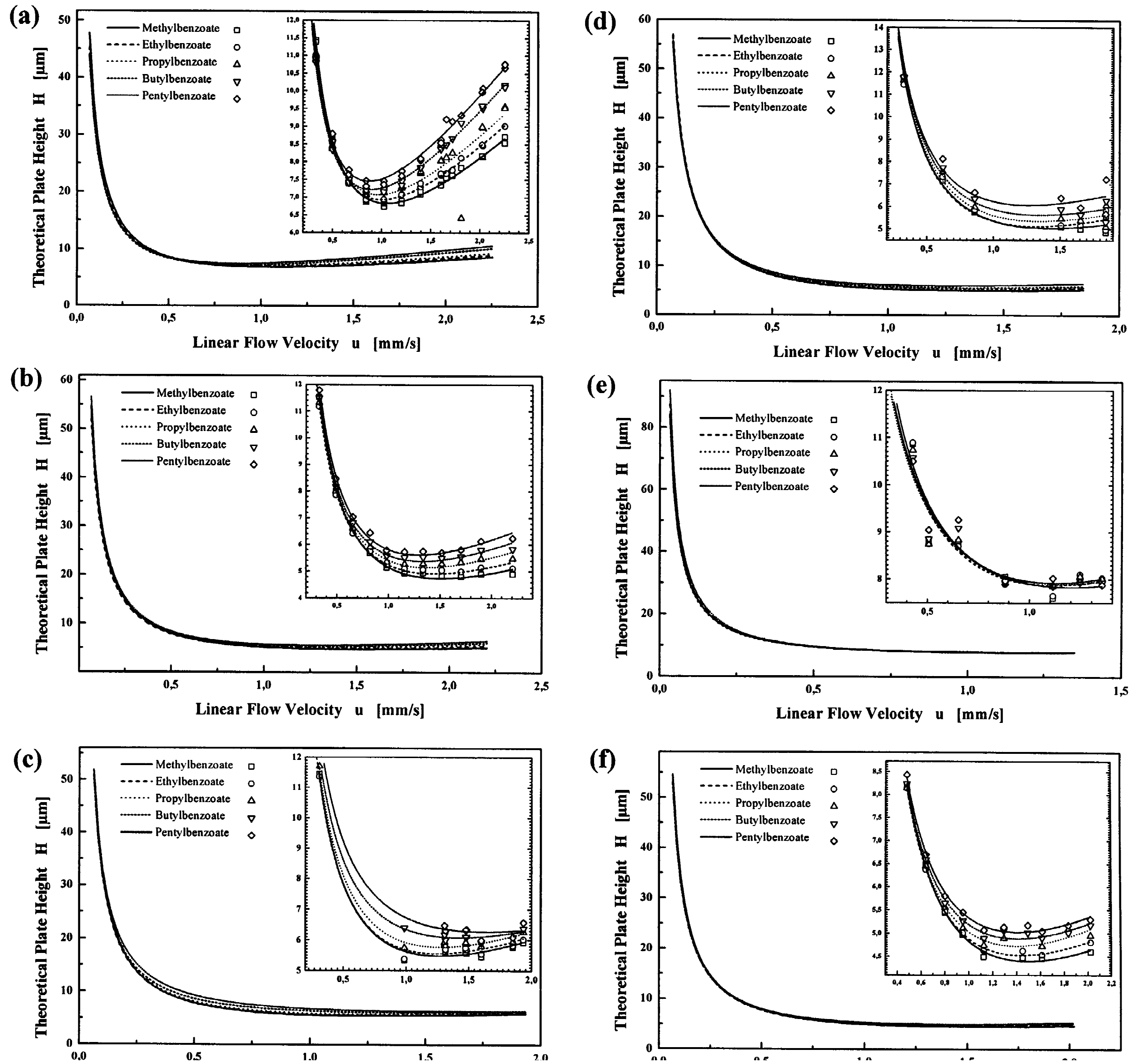

Fig. 5. Van Deemter plots of various capillary columns. Injection: 3 kV, 3 s. Applied voltage: values 1–30 kV. Detection at 224 nm. Stationary phase: Grom-Sil ODS-0 AB, $d_P = 3$ µm. Other conditions are described in Sections 2.2. and 3.4. (a) Van Deemter plots of a single-frit column set-up. Packed segment 100 µm I.D., open segment 75 µm I.D., outlet taper 27.5 µm I.D. Effective length 25 cm, total length 37 cm, detection 2.0 cm after column. (b) Van Deemter plots of a single-frit column set-up. Packed segment 100 µm I.D., open segment 50 µm I.D., outlet taper 27.5 µm I.D. Effective length 25 cm, total length 37 cm, detection 2.0 cm after column. (c) Van Deemter plots of a single-frit column set-up. Packed segment 150 µm I.D., open segment 75 µm I.D., outlet taper 22.0 µm I.D. Effective length 25 cm, total length 37 cm, detection 2.0 cm after column. (d) Van Deemter plots of a single-frit column set-up. Packed segment 100 µm I.D., open segment 50 µm I.D., outlet taper 20.0 µm I.D. Effective length 25 cm, total length 35.5 cm, detection 0.5 cm after column. (e) Van Deemter plots of a single-frit column set-up with bubble cell. Packed segment 100 µm I.D., open segment 30 µm I.D. No outlet taper. Effective length 25 cm, total length 37.5 cm, detection 2.5 cm after column. (f) Van Deemter plots of a fritless column set-up. Packed segment 100 µm I.D., open segment 50 µm I.D., inlet taper 22.0 µm I.D., outlet taper 26.0 µm I.D. Effective length 25 cm, total length 37 cm, detection 2.0 cm after column.

[11] P. Gfrörer, J. Schewitz, K. Puseker, E. Bayer, Anal. Chem. 4 (1999) 315A.
[12] S.E. Van den Bosch, S. Heemstra, J.C. Kraak, H. Poppe, J. Chromatogr. A 755 (1996) 165.
[13] N.W. Smith, M.B. Evans, Chromatographia 38 (1994) 649.
[14] R.J. Boughtflower, T. Underwood, C.J. Paterson, Chromatographia 40 (1995) 329.
[15] H. Alborn, G. Stenhagen, J. Chromatogr. 323 (1985) 47.
[16] G.A. Lord, D.B. Gordon, P. Myers, B.W. King, J. Chromatogr. A 768 (1997) 9.
[17] G. Choudhary, C. Horváth, J.F. Banks, J. Chromatogr. A 828 (1998) 469.
[18] R.A. Carney, M.M. Robson, K.D. Bartle, P. Myers, J. High Resolut. Chromatogr. 22 (1999) 29.
[19] B. Behnke, G. Schlotterbeck, U. Tallarek, S. Strohschein, L.-H. Tseng, T. Keller, K. Albert, E. Bayer, Anal. Chem. 68 (1996) 1110.
[20] K. Puseker, J. Schewitz, P. Gfrörer, L.-H. Tseng, K. Albert, E. Bayer, Anal. Chem. 70 (1998) 3280.
[21] P. Gfrörer, J. Schewitz, K. Puseker, L.-H. Tseng, K. Albert, E. Bayer, Electrophoresis 20 (1999) 3.
[22] C. Rentel, P. Gfrörer, E. Bayer, Electrophoresis 20 (1999) 2329.
[23] G. Guiochon, S. Golshan-Shirazi, A.M. Katti, Fundamentals of Preparative and Nonlinear Chromatography, Academic Press, Boston, MA, 1994.
[24] A.S. Rathore, Cs. Horváth, Anal. Chem. 70 (1998) 3069.